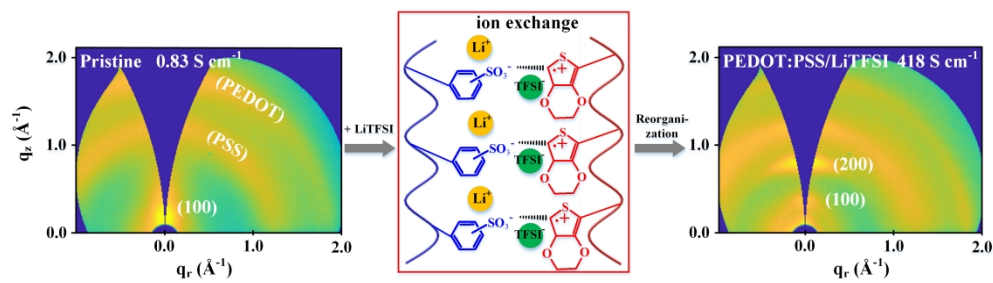


This document is confidential and is proprietary to the American Chemical Society and its authors. Do not copy or disclose without written permission. If you have received this item in error, notify the sender and delete all copies.

### Effects of cationic species in salts on the electrical conductivity of doped PEDOT:PSS films

Journal:	<i>ACS Applied Polymer Materials</i>
Manuscript ID	Draft
Manuscript Type:	Letter
Date Submitted by the Author:	n/a
Complete List of Authors:	Li, Xin; Sun Yat-Sen University, School of Materials Science and Engineering, PCFM Lab Liu, Zhen; Sun Yat-Sen University Zhou, Zekun; Sun Yat-Sen University, School of Materials Science and Engineering Gao, Haiyang; Sun Yat-Sen University, School of Materials Science and Engineering Liang, Guo Dong; Sun Yat-Sen University, PCFM and GDHPPC labs, School of Materials Science and Engineering Rauber, Daniel; Universitat des Saarlandes, Chemistry Kay, Christopher; Saarland University Zhang, Peng; Sun Yat-Sen University, School of Materials Science and Engineering

SCHOLARONE™  
Manuscripts



Abstract Graphic

341x96mm (300 x 300 DPI)

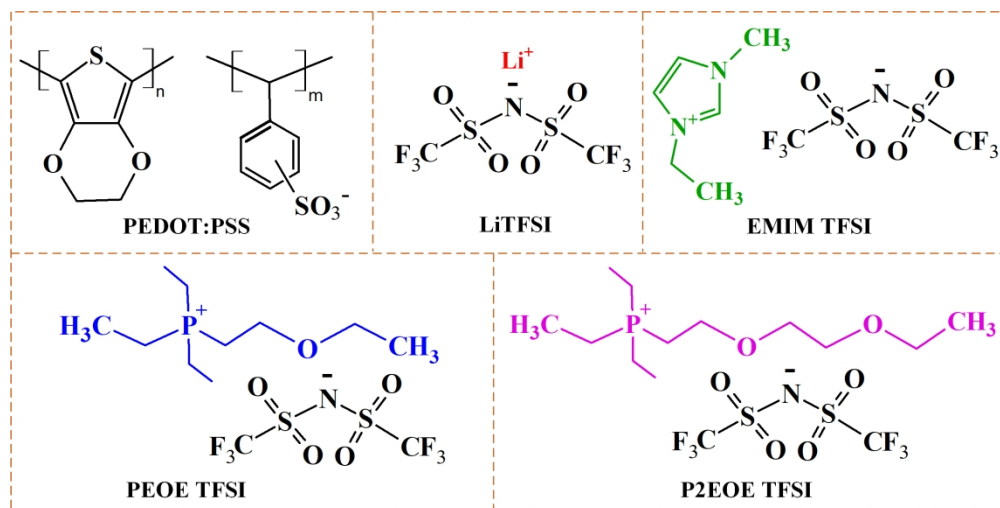


Figure 1. Chemical structure of PEDOT:PSS and ionic salts used in this work.

202x101mm (300 x 300 DPI)

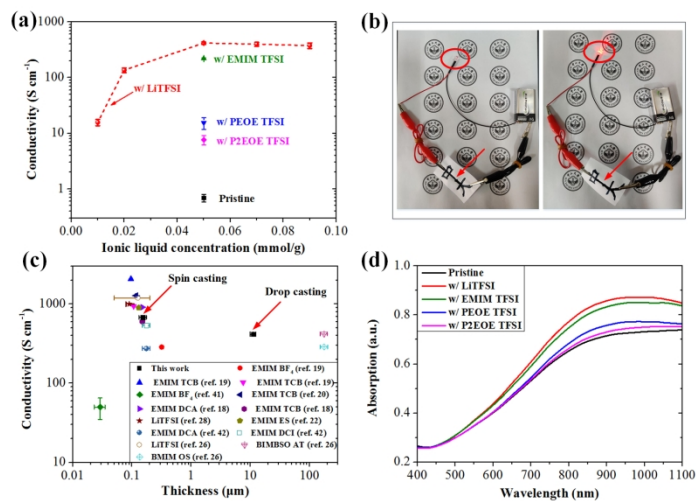


Figure 2. (a) The electrical conductivity result of PEDOT:PSS films doped with different ILs and LiTFSI at a series of concentration. (b) Photo images of LED electrical circuits and the parts for PEDOT:PSS composite deposited on paper are marked with the arrows (left: PEDOT:PSS, right: PEDOT:PSS/LiTFSI composite). (c) Thickness influence on the conductivity of PEDOT:PSS film (our work is marked by the arrows). (d) UV-Vis absorption spectra of pristine PEDOT:PSS and PEDOT:PSS/IL dispersion. Notes: PEDOT:PSS/salt is denoted as w/salt, mmol/g represents the stoichiometry of salts in 1.0 g of PEDOT: PSS water dispersion.

202x101mm (300 x 300 DPI)

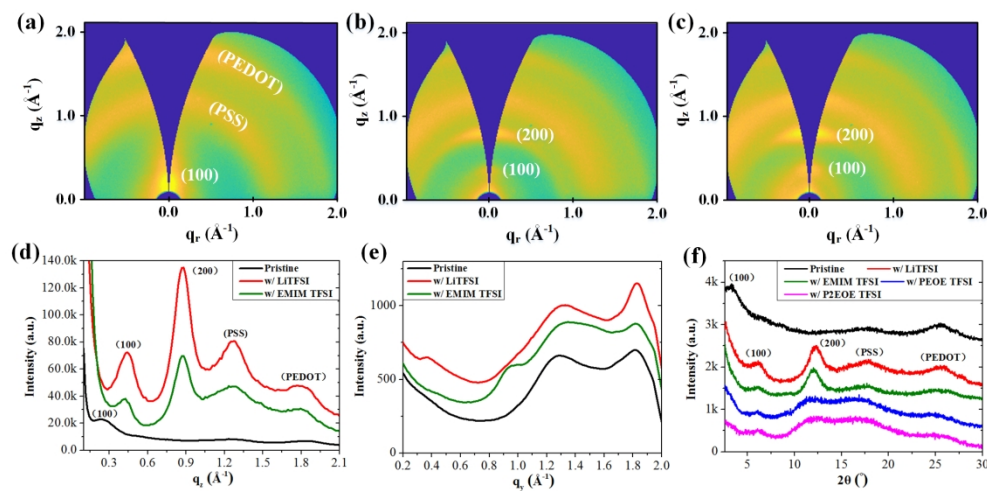


Figure 3. Typical two-dimensional GIWAXS patterns of (a) pristine, (b) EMIM TFSI-treated and (c) LiTFSI-treated PEDOT:PSS films. (d) Vertical cake cuts of the initial GIWAXS data of pristine and salt-treated PEDOT:PSS films. (e) Horizontal cake cuts of the initial GIWAXS data of pristine and salt-treated PEDOT:PSS films. (f) GIXRD data of pristine and salt-treated PEDOT:PSS films. Note: PEDOT:PSS/salt is denoted as w/salt.

202x101mm (300 x 300 DPI)

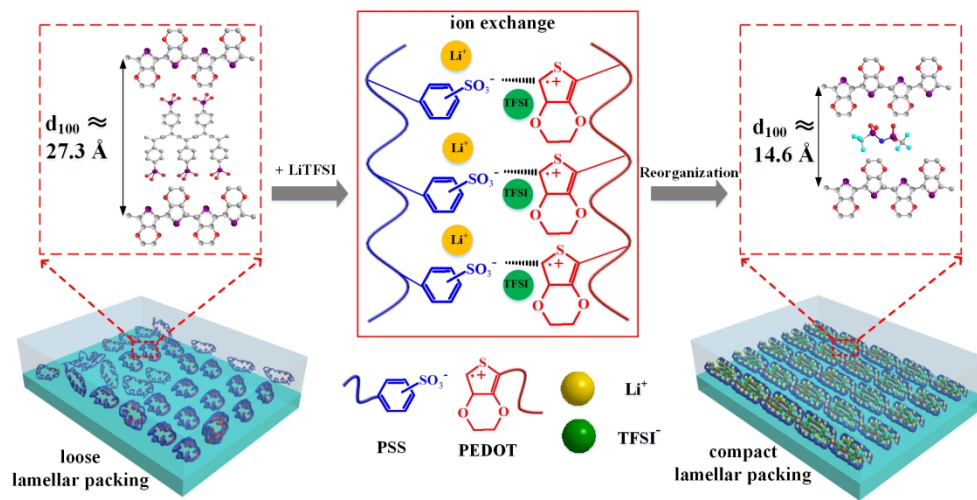


Figure 4. Schematic illustration of the structure of polymer composite film: loose lamellar packing of pristine PEDOT:PSS (left) and compacted lamellar packing of PEDOT:PSS /LiTFSI composite (right).

202x101mm (300 x 300 DPI)

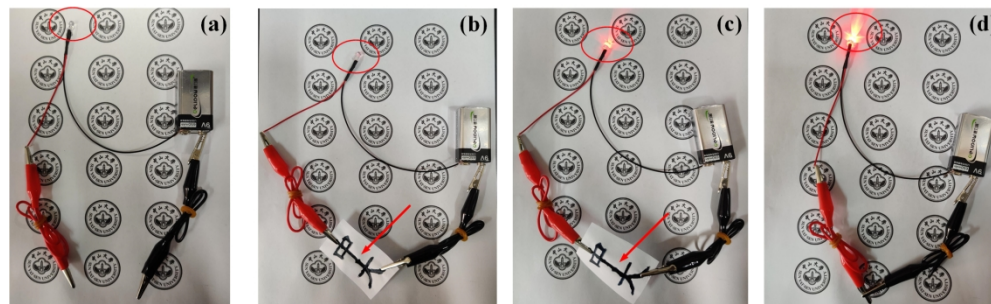


Figure S1. Photo images of LED electrical circuits and the parts for PEDOT:PSS composite deposited on paper are marked with the arrows; (a) Open circuit, (b) Pristine film, (c) PEDOT:PSS/LiTFSI composite, (d) Wire connection only.

202x101mm (300 x 300 DPI)

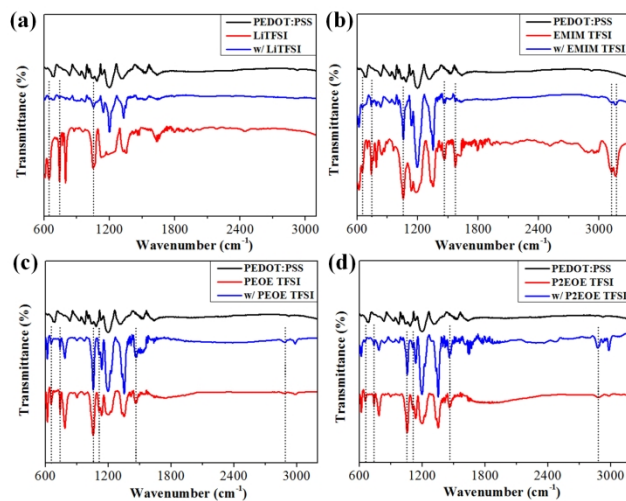


Figure S2. FTIR spectra of pristine film, pure salts and PEDOT:PSS films treated with salts (a) LiTFSI, (b) EMIM TFSI, (c) PEOE TFSI, (d) P2EOE TFSI.

202x101mm (300 x 300 DPI)

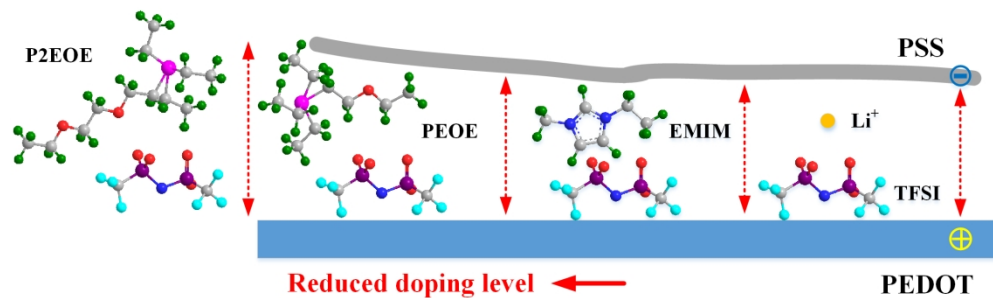


Figure S3. Schematic diagram of cationic size effect of the electrostatic interaction of PEDOT:PSS and salts.

202x101mm (300 x 300 DPI)

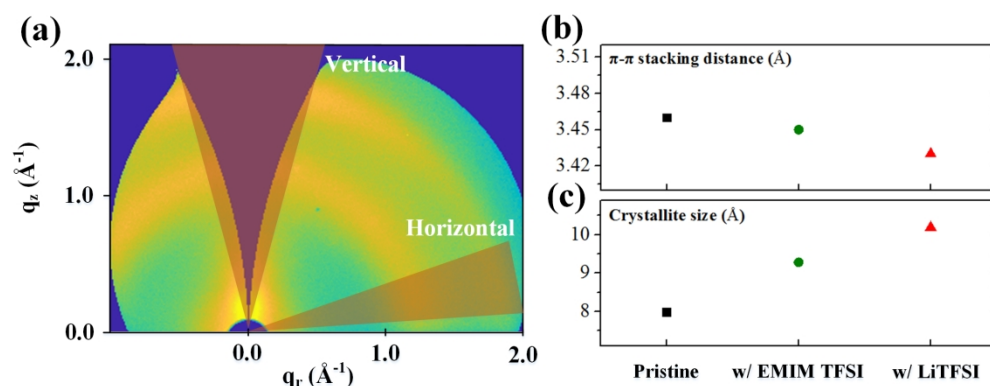


Figure S4. (a) Exemplary vertical cake cut of  $\chi = -16^\circ$ – $16^\circ$  and horizontal cake cut of  $\chi = 70^\circ$ – $85^\circ$  on pristine PEDOT:PSS. (b)  $\pi$ - $\pi$  stacking distance of horizontal oriented PEDOT crystallites. (c) Apparent crystallite size of horizontal oriented PEDOT.

202x101mm (300 x 300 DPI)

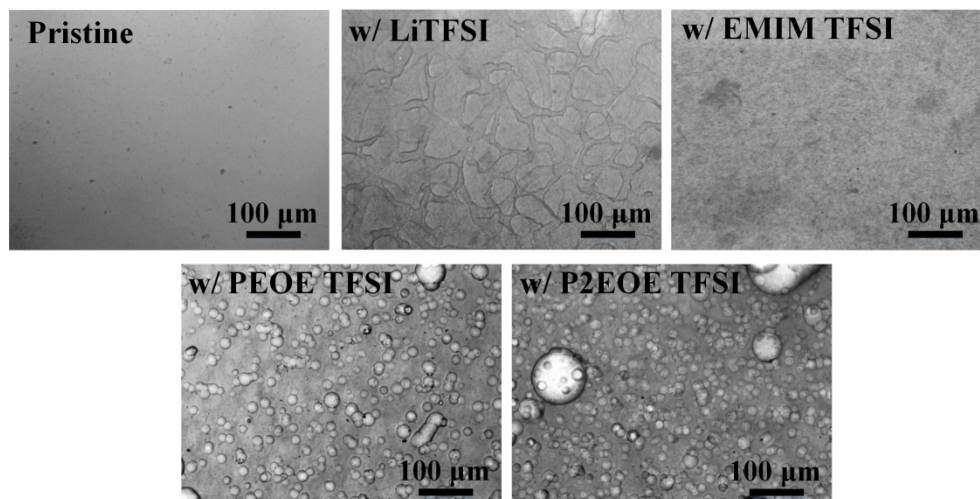


Figure S5. Optical microscope images of PEDOT/PSS films treated with various ionic additives. Note: PEDOT:PSS/salt is denoted as w/salt.

202x101mm (300 x 300 DPI)

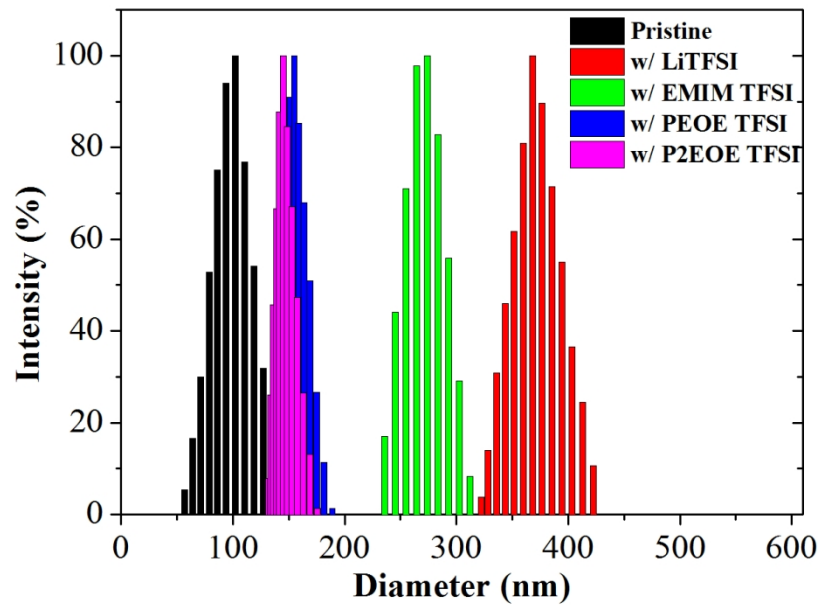


Figure S6. Dynamic light scattering (DLS) data of PEDOT:PSS and salt-mixed PEDOT:PSS dispersions.

127x89mm (300 x 300 DPI)

# Effects of cationic species in salts on the electrical conductivity of doped PEDOT:PSS films

Xin Li<sup>a</sup>, Zhen Liu<sup>a</sup>, Zekun Zhou<sup>a</sup>, Haiyang Gao<sup>a</sup>, Guodong Liang<sup>a</sup>, Daniel Rauber<sup>b</sup>,  
Christopher Kay<sup>b</sup>, Peng Zhang<sup>a,\*</sup>

<sup>a</sup> School of Materials Science and Engineering, PCFM Lab, Sun Yat-sen University, Guangzhou  
510275, China

<sup>b</sup> Department of Chemistry, Saarland University, 66123, Saarbrücken, Germany

Corresponding authors: Peng Zhang, E-mail: [zhangpeng3@mail.sysu.edu.cn](mailto:zhangpeng3@mail.sysu.edu.cn)

## Abstract

The influence of chemical composition of the doping salts on the conductivity of the poly(3,4-ethylenedioxythiophene):poly(styrenesulfonate) (PEDOT:PSS) films was studied in this work. A series of salts with different cations but the same anion were mixed with PEDOT:PSS. We found out that doping salts of small-size cations led to better conductivity due to the improved crystalline ordering of PEDOT, as revealed by the grazing-incidence wide-angle X-ray scattering (GIWAXS) data. This phenomenon can be rationalized with the fact that small-size cations can dissociate the PSS from PEDOT due to stronger Coulomb interactions, leading to rearrangement of the PEDOT. These findings will help to develop new recipes based on the PEDOT:PSS/salt composite towards the applications for printed flexible electronics, portable displays and flexible energy storage devices.

In the past decade, the stretchable flexible electronics have developed fast as essential parts of the popular electronic devices.<sup>1-3</sup> In these applications, conductive polymers have received tremendous attention as ideal electrodes to replace the traditional indium tin oxide (ITO) ones due to their excellent mechanical properties (i.e., flexibility) and solution

1  
2  
3  
4 processability. In particular, poly(3,4-ethylenedioxythiophene):poly(styrenesulfonate)  
5  
6 (PEDOT:PSS) is recognized as the most promising candidate owing to its mechanical  
7  
8 flexibility, visible-light transmittance, biocompatibility, solution processability and good  
9  
10 environmental stability.<sup>4-6</sup> However, untreated PEDOT:PSS film displays poor electrical  
11  
12 conductivity as low as about  $1 \text{ S cm}^{-1}$ , limiting its practical application in popular electronic  
13  
14 devices. The low conductivity is mainly attributed to the existence of insulating PSS chains  
15  
16 that wrap the conductive PEDOT core and inhibit the formation of PEDOT conductive  
17  
18 network.<sup>7-9</sup> To solve this issue, secondary doping agents like acids,<sup>10,11</sup> surfactants,<sup>12</sup> organic  
19  
20 solvents<sup>13-15</sup> and recently the ionic salts<sup>16-22</sup> are generally introduced into PEDOT:PSS to  
21  
22 achieve conductivity that is comparable to the commercial ITO products. Especially the ionic  
23  
24 salts in solid or liquid form have garnered particular interest due to their high thermal  
25  
26 stability,<sup>23</sup> unique structural<sup>24</sup> and electrochemical properties,<sup>25</sup> as well as an ability to  
27  
28 improve conductivity and stretchability of PEDOT:PSS films.<sup>20,26</sup>

29  
30  
31  
32  
33  
34  
35  
36  
37  
38  
39 Recent studies indicate that ionic interaction between salts and PEDOT:PSS promoted  
40  
41 microstructure reorganization which resulted in the formation of PEDOT-rich and PSS-rich  
42  
43 microdomains. This eased the formation of interconnected PEDOT networks, resulting in  
44  
45 higher electrical conductivities.<sup>27-29</sup> For example, Badre et al.<sup>19</sup> reported the conductivity of  
46  
47 PEDOT:PSS composite with 1-ethyl-3-methylimidazolium tetracyanoborate (EMIM TCB)  
48  
49 was  $2084 \text{ S cm}^{-1}$  which derived from the salt-induced charge screening between PEDOT and  
50  
51 PSS and was three orders of magnitude higher than that of pristine PEDOT:PSS film. Li et  
52  
53 al.<sup>28</sup> revealed ionic exchange between bis(trifluoromethanesulfonyl)imide lithium salt  
54  
55  
56  
57  
58  
59  
60

(LiTFSI) and PEDOT:PSS ( $\text{LiTFSI} + \text{PEDOT:PSS} = \text{PEDOT:TFSI} + \text{Li:PSS}$ ) induced PEDOT microdomain converged together to form a packed and interconnected net structure, which synergistically enhanced the thermoelectric and mechanical performances. Similar ion exchange process and microstructure reorganization was reported by Kee et al.<sup>30</sup> in the composite of PEDOT:PSS with a series of EMIM cation based ionic liquids (ILs). For an in-depth structural analysis, grazing-incidence wide-angle X-ray scattering (GIWAXS) measurement was employed and disclosed a highly ordered nanofibrillar structures of PEDOT chains that eased the electron transfer. Meanwhile, plenty of recent work have focused on studying the structure-performance relationship in the PEDOT:PSS/salt composites to tune the macroscopic conductivity with molecular designs. It's generally summarized that chemical composition of the salts had strong influence on the conductivity of the PEDOT:PSS/salt composites. Ambroise et al. have claimed that ion exchange ( $\text{EMIM:anion} + \text{PEDOT:PSS} = \text{EMIM:PSS} + \text{PEDOT:anion}$ , i.e., anionic effect) released the PEDOT from the coupling with PSS, which provided the PEDOT higher *p*-doping density and improved conductivity.<sup>31</sup> However, to the best of our knowledge, the influence of the cations on the structure and conductivity of PEDOT:PSS films have not been explored yet.

In order to investigate the effect of different cationic species on the structure and conductivity of PEDOT:PSS (Orgacon Dry, Agfa Gevaert N.V., Belgium), we chose four salts with various cations, including lithium ( $\text{Li}^+$ ), 1-ethyl-3-methylimidazolium (EMIM), (2-ethoxyethyl)triethylphosphonium (PEOE) and (2-(2-ethoxyethoxy)ethyl)triethylphosphonium (P2EOE), but the same

bis(trifluoromethanesulfonyl)amide (TFSI) anion, as demonstrated in Figure 1. For the preparation of PEDOT:PSS/IL composite, 0.05 mmol salt was added into 1000 mg PEDOT:PSS aqueous dispersion (1.6 wt%), under vigorous stirring.

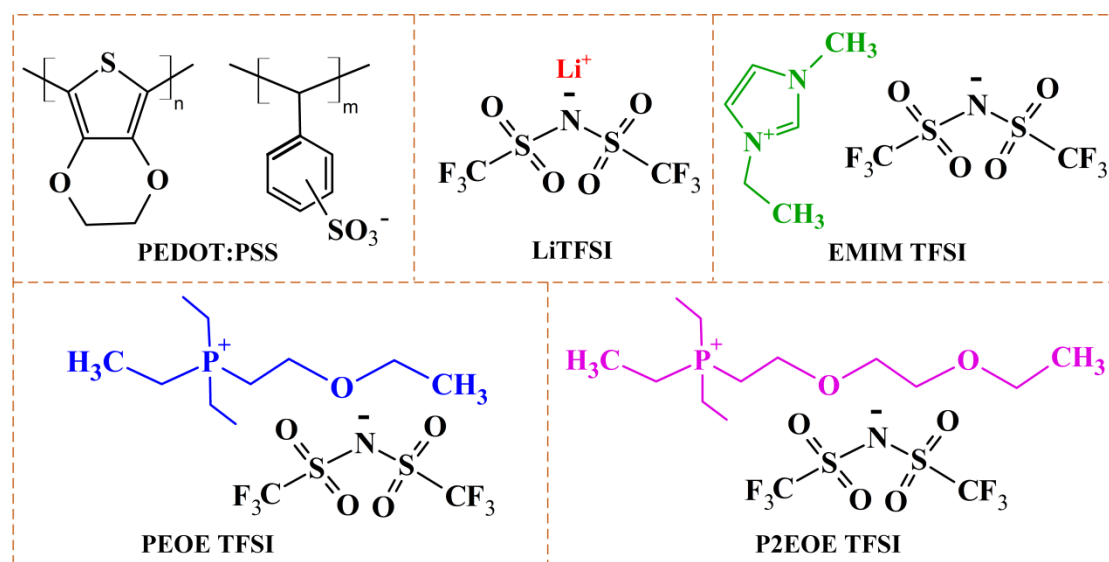


**Figure 1.** Chemical structure of PEDOT:PSS and ionic salts used in this work.

We chose TFSI as the anion because it was illustrated to be effective for the improvement of the PEDOT conductivity.<sup>32</sup> The cationic size increases monotonically along this series,  $\text{Li}^+ < \text{EMIM} < \text{PEOE} < \text{P2EOE}$ . Meanwhile, these cations were widely used as aqueous electrolyte materials in the previous studies and the self-diffusion coefficients for lithium, EMIM, PEOE and P2EOE cations are  $\sim 10 \times 10^{-11}$ ,<sup>33,34</sup>  $\sim 7 \times 10^{-11}$ ,<sup>35</sup>  $2.33 \times 10^{-11}$  and  $2.30 \times 10^{-11} \text{ m}^2 \text{ S}^{-1}$ ,<sup>36</sup> respectively. Thus, we can infer that small-size cation showed stronger mobility in PEDOT:PSS aqueous dispersion. The fast mobility of cation helps to combine with PSS anion to form the coupled cation:PSS and screens the Coulomb interaction between PEDOT and PSS. It's expected that salt with small size and high cationic mobility would change significantly the molecular structure and thus the conductivity of PEDOT:PSS/salt in the dried films.

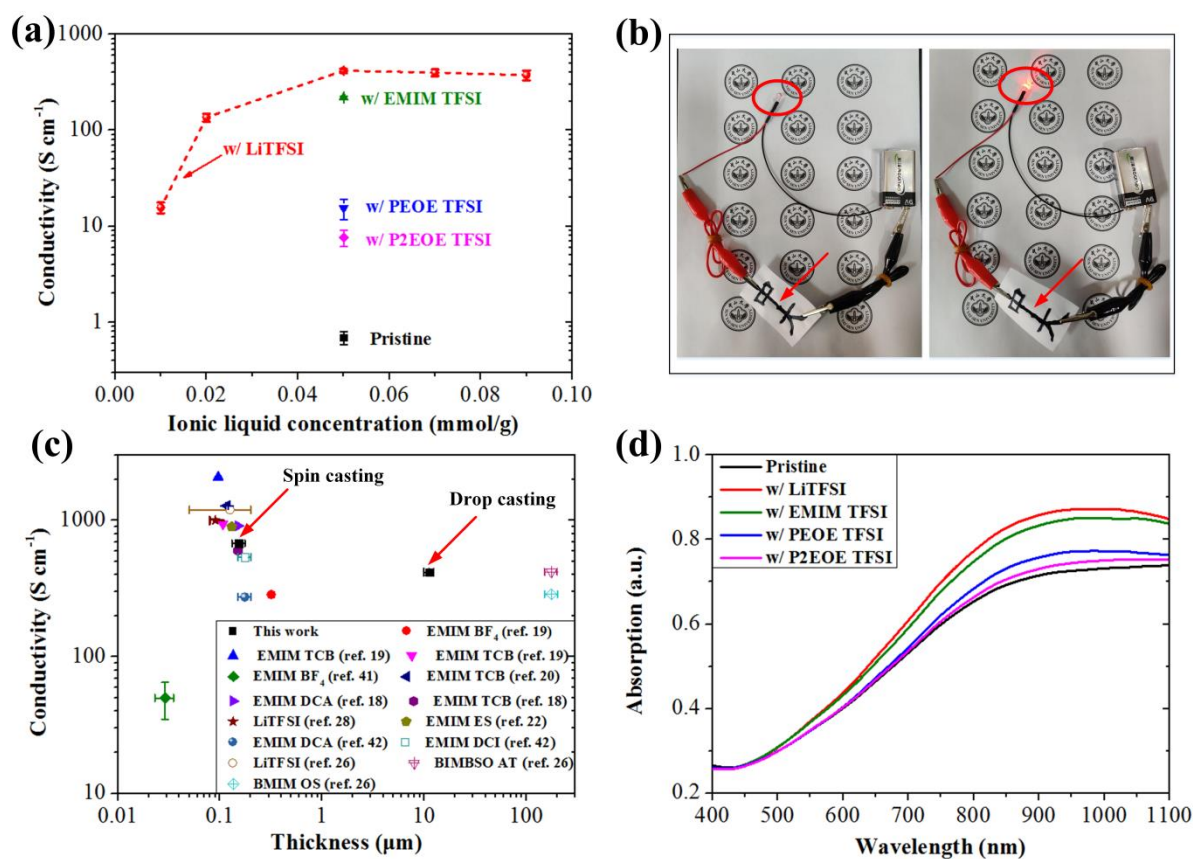


**Figure 2.** (a) The electrical conductivity result of PEDOT:PSS films doped with different ILs and LiTFSI at a series of concentration. (b) Photo images of LED electrical circuits and the parts for PEDOT:PSS composite deposited on paper are marked with the arrows (left: PEDOT:PSS, right: PEDOT:PSS/LiTFSI composite). (c) Thickness influence on the conductivity of PEDOT:PSS film (our work is marked by the arrows). (d) UV-Vis absorption spectra of pristine PEDOT:PSS and PEDOT:PSS/IL dispersion. Notes: PEDOT:PSS/salt is denoted as w/salt, mmol/g represents the stoichiometry of salts in 1.0 g of PEDOT: PSS water dispersion.

To verify our hypothesis, we deposited the sample on glass substrate and measured the conductivity of dried films with a multimeter (ST-2258A, Suzhou Jingge Electronic Co., Ltd.) and four-probe method at ca. 58% relative humidity. By taking the PEDOT:PSS/LiTFSI composite sample as an example, we found that the electrical conductivity of the composite peaked at sample with 0.05 mmol/g salt (Figure 2a) and this hybrid sample was used in the

1  
2  
3  
4 following work. As shown in Figure 2a, the electrical conductivity of PEDOT:PSS films  
5  
6 increased after doping with salts. It should be noted that neat salts did not show detectable  
7  
8 electrical conductivity. The pristine PEDOT:PSS sample shows a conductivity of  $0.83 \text{ S cm}^{-1}$ ,  
9  
10 while the conductivity values for polymer composite with  $\text{Li}^+$ , EMIM, PEOE and P2EOE are  
11  
12 418.06, 220.00 15.50 and  $7.63 \text{ S cm}^{-1}$ , respectively (cf. Table S1 of the supporting  
13  
14 information). The enhanced conductivity through mixing with salts is consistent with the  
15  
16 previous reports.<sup>37-40</sup> In addition, there is an obvious difference in the conductivity for the  
17  
18 PEDOT:PSS/salt with different cationic components. The smaller-size cations with faster ion  
19  
20 diffusivity ( $\text{Li}^+$  and EMIM) show better conductivity. Recent work about the mixture of  
21  
22 PEDOT:PSS and EMIM TCB has demonstrated that the IL triggered the structural  
23  
24 reorganization via ion exchange, i.e.,  $\text{cation:anion} + \text{PEDOT:PSS} \rightleftharpoons \text{PEDOT:anion} +$   
25  
26  $\text{cation:PSS}$ , leading to the formation of highly ordered nanofibrillar structures of PEDOT  
27  
28 chains and an enhancement of electrical conductivity.<sup>28-30</sup> We infer that the small-size cations  
29  
30 do ion exchange with PEDOT:PSS that lead to a higher conductivity value in  
31  
32 PEDOT:PSS/salt.  
33  
34  
35  
36  
37  
38  
39  
40  
41  
42  
43  
44

45 To demonstrate the conductivity improvement, we drop casted PEDOT:PSS ink on paper  
46  
47 and dried it as a part of the electrical circuit of light-emitting diode (LED), as shown in Figure  
48  
49 2b and Figure S1. We found the LED with a PEDOT:PSS/salt circuit was much brighter than  
50  
51 the PEDOT:PSS one, confirming the high conductivity of salt-doped PEDOT:PSS and  
52  
53 demonstrating its potential application in printed flexible electronics. Moreover, we figured  
54  
55 out that the conductivity value of PEDOT:PSS/LiTFSI in this work is comparable to those of  
56  
57  
58  
59  
60

1  
2  
3  
4 PEDOT:PSS/salts mentioned in the previous reports,<sup>16,18,19,26,41,42</sup> see Figure 2c, Table S2 and  
5  
6 Table S3 of the supporting information. Note: some deviations are attributed to the sample  
7  
8 preparation method and film thickness because our work (Figure 2c) and the others' reports  
9  
10 show that spin-casted nanometer films has better conductivity than the drop-casted  
11  
12 micrometer ones.<sup>26</sup>  
13  
14  
15  
16

17 Previous studies indicate that ion exchange reaction between PEDOT:PSS and ILs  
18  
19 increased the oxidation state of the PEDOT polymer chains and thus the electronic  
20  
21 conductivity.<sup>18,29</sup> We characterized the oxidation level of PEDOT:PSS with a SHI-MADZU  
22  
23 UV-3600 spectrophotometer. As shown in Figure 2d, the broad absorption band near 850 nm  
24  
25 is attributed to oxidation state of PEDOT, i.e., the single polaron with a positive charge.<sup>42-44</sup>  
26  
27  
28 By referring to this peak, we found that PEDOT:PSS/salts films showed a much stronger  
29  
30 absorption than PEDOT:PSS, corresponding to an enhanced oxidation level (i.e., higher  
31  
32 *p*-doping density) of PEDOT chains.<sup>29</sup> The PEDOT conductivity is primarily dependent on  
33  
34 the positive charges located along the polymer backbone.<sup>39,45</sup> Thus the electrical conductivity  
35  
36 of PEDOT is proportional to the level of *p*-doping. Indeed, the conductivity descends along  
37  
38 the series, PEDOT:PSS/LiTFSI, PEDOT:PSS/EMIM TFSI, PEDOT:PSS/PEOE TFSI,  
39  
40 PEDOT:PSS/P2EOE TFSI and pristine PEDOT:PSS, which can be rationalized with a lower  
41  
42 *p*-doped level. Furthermore, there is an obvious difference on the *p*-doped level in  
43  
44 PEDOT:PSS/salts. The composite with small cations show high-density *p*-doping. This  
45  
46 phenomenon is likely derived from the fact that cations with fast mobility are easier to  
47  
48 combine with negatively-charged PSS molecules and leave a significant amount of TFSI  
49  
50  
51  
52  
53  
54  
55  
56  
57  
58  
59  
60

anions for the PEDOT (cf. Figure S2). By referring to the previous reports,<sup>31,46</sup> we hypothesize that TFSI anions take the role of PSS anions to weaken the screening effects of original PSS anions on PEDOT, thus the oxidized PEDOT<sup>+</sup> cations release from the shielding effect of PSS<sup>-</sup> and sustain their *p*-doped states. In contrast, the salts with big size and slow cationic mobility such as PEOE and P2EOE could not combine with the PSS<sup>-</sup> as efficient as that of Li<sup>+</sup> due to the steric effect (cf. Figure S3).

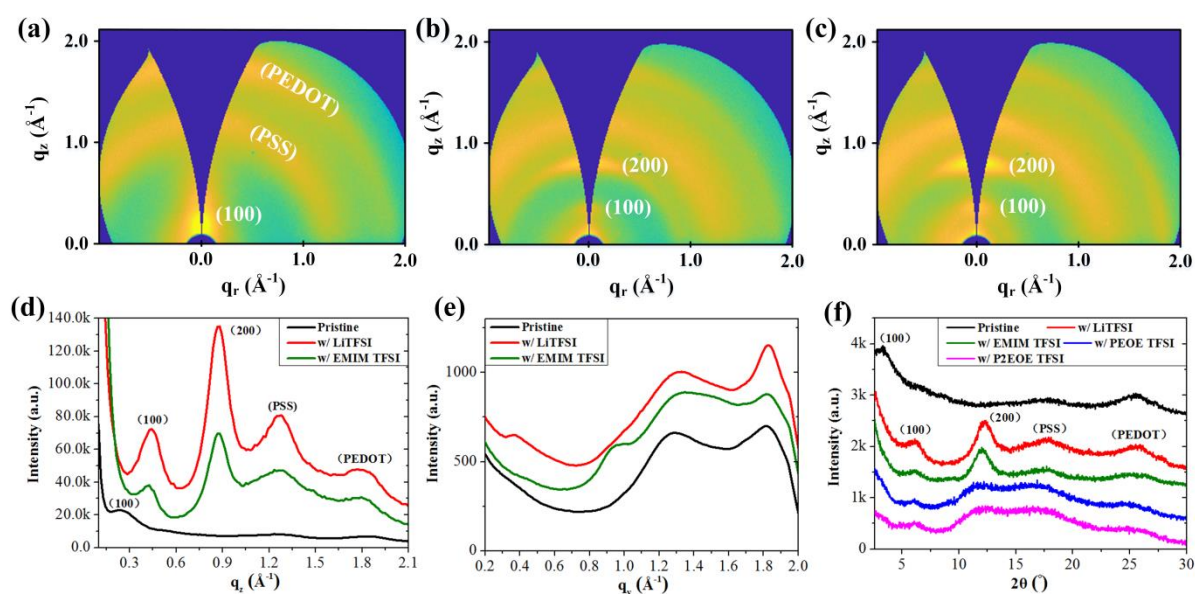


**Figure 3.** Typical two-dimensional GIWAXS patterns of (a) pristine, (b) EMIM TFSI-treated and (c) LiTFSI-treated PEDOT:PSS films. (d) Vertical cake cuts of the initial GIWAXS data of pristine and salt-treated PEDOT:PSS films. (e) Horizontal cake cuts of the initial GIWAXS data of pristine and salt-treated PEDOT:PSS films. (f) GIXRD data of pristine and salt-treated PEDOT:PSS films. Note: PEDOT:PSS/salt is denoted as w/salt.

In the following, we explore the structure-property relationships of PEDOT:PSS/salt composite with a series of complementary tools. The microstructure of PEDOT:PSS composite films was characterized with GIWAXS based on synchrotron light at 1W1A beamline of BSRF, Beijing, China (cf. supporting information). GIWAXS is a

1  
2  
3  
4 well-established protocol to characterize the surface and interface structures of polymer thin  
5  
6 film,<sup>47-49</sup> including PEDOT:PSS before and after IL doping. For example, Kee et al.<sup>30</sup>  
7  
8 demonstrated a highly ordered nanofibrillar structures of PEDOT and Saxena et al.<sup>18</sup> reported  
9  
10 a shortened  $\pi$ - $\pi$  stacking distance between PEDOT molecules upon salts' doping. Such  
11  
12 structure change leads to an enhanced conductivity of the PEDOT hybrid sample. The sample  
13  
14 dispersion was deposited on silicon substrate ((100) orientation, PlutoSemi Co., Ltd) and the  
15  
16 thickness of the dried film was around 11  $\mu\text{m}$ , measured by an Ambios XP-1 profilometer.  
17  
18 Figure 3a-c show the typical 2D scattering pattern of GIWAXS. In Figure 3a, three  
19  
20 characteristic peaks with  $q = 0.23 \text{ \AA}^{-1}$  ( $d = 27.3 \text{ \AA}$  calculated with  $d=2\pi/q$ ),  $1.26 \text{ \AA}^{-1}$  ( $d = 5.0$   
21  
22  $\text{\AA}$ ), and  $1.82 \text{ \AA}^{-1}$  ( $d = 3.4 \text{ \AA}$ ) are attributed to alternating stacking of PEDOT and PSS (i.e.,  
23  
24 PEDOT (100) crystal planes),  $\pi$ - $\pi$  stacking of PSS, and  $\pi$ - $\pi$  stacking of PEDOT,  
25  
26 respectively.<sup>7,50</sup> The lattice spacing distance of (100) plane ( $d_{100}$ ) for pristine PEDOT:PSS is  
27  
28  $27.3 \text{ \AA}$ , which decreases to  $15.0$  and  $14.6 \text{ \AA}$  for PEDOT:PSS/EMIM TFSI and  
29  
30 PEDOT:PSS/LiTFSI composite films, respectively (Figure 3d). The decreased  $d_{100}$  value  
31  
32 means a shorter  $\pi$ - $\pi$  stacking distance and improved crystalline ordering along the main chain  
33  
34 direction.<sup>51</sup> Additionally, a new peak corresponding to (200) crystal plane of PEDOT is found  
35  
36 at  $q = 0.87 \text{ \AA}^{-1}$  ( $d = 7.2 \text{ \AA}$ ) (Figure 3b-d), indicating an enhanced long-range order of PEDOT  
37  
38 crystals after salt doping.<sup>52</sup> In addition, we studied the in-plane molecular structure of  
39  
40 PEDOT:PSS hybrid film by referring to the horizontal cake cuts (Figure 3e) of the initial  
41  
42 GIWAXS data. A shortened PEDOT  $\pi$ - $\pi$  stacking distance and an improved PEDOT  
43  
44 crystallite size in horizontal direction (cf. Figure S4b and S4c) upon the salt doping further  
45  
46  
47  
48  
49  
50  
51  
52  
53  
54  
55  
56  
57  
58  
59  
60

1  
2  
3  
4 confirms an enhanced crystalline ordering of PEDOT.<sup>52</sup> In the PEDOT:PSS composite, carrier  
5  
6 mobility depends upon the intermolecular charge transfer rate in the  $\pi$ - $\pi$  stacking  
7  
8 direction.<sup>51,53</sup> Namely, more ordered and densely packed PEDOT crystallites in this direction  
9  
10 will aid electron transport thereby improve the conductivity. Indeed, the highest conductivity  
11  
12 of LiTFSI-treated PEDOT:PSS can be rationalized with the structure changes disclosed by  
13  
14 GIWAXS measurements. Similar diffraction results have been reported in highly conductive  
15  
16 PEDOT:PSS by Kim et al.<sup>8</sup> who illustrated that ion exchange between concentrated H<sub>2</sub>SO<sub>4</sub>  
17  
18 and PEDOT:PSS generated a highly ordered and densely packed PEDOT:PSS nanofibril  
19  
20 structure. Moreover, the salt-mixing induced conductivity change agrees with the large-scale  
21  
22 structure change as observed with optical microscope (cf. Figure S5). In general,  
23  
24 LiTFSI-treated PEDOT:PSS shows clear interconnected networks, which might serve as  
25  
26 conductive path and ease the electron transport. Thus, we summarize that the well-aligned and  
27  
28 interconnected PEDOT domains in the PEDOT:PSS/salt composite resulted in a high  
29  
30 conductivity compared to that of the pristine PEDOT:PSS.  
31  
32  
33  
34  
35  
36  
37  
38  
39  
40  
41

42 To illustrate the generality of the relationship between crystalline structure and  
43  
44 conductivity in PEDOT:PSS films mentioned above, the crystalline structure of all four  
45  
46 PEDOT:PSS/salt composite films were measured with GIXRD (Bruker D8 Advance,  
47  
48 Germany). As shown in the Figure 3f, the curve of pristine PEDOT:PSS film shows three  
49  
50 characteristic peaks:  $2\theta = 3.3^\circ$  ( $q = 0.23 \text{ \AA}^{-1}$ ),  $17.7^\circ$  ( $q = 1.26 \text{ \AA}^{-1}$ ), and  $25.8^\circ$  ( $q = 1.82 \text{ \AA}^{-1}$ ),  
51  
52 which are consistent with the GIWAXS data. In addition, the PEDOT:PSS/salt composites  
53  
54 show an additional (200) peak and enhanced scattering intensity, like the GIWAXS results.  
55  
56  
57  
58  
59  
60

Both the GIWAXS and GIXRD results indicate that the improved conductivity of PEDOT:PSS film after doping with salts originates from an enhanced crystalline ordering, agreeing with the previous reports.<sup>18,20,42,53</sup> We understand the structure change with the facts that the salt anion can play the role of condensing agent for polyelectrolytes such as negatively charged DNA,<sup>54</sup> i.e., salts hold the *p*-doped PEDOT chains together at a shorter  $\pi$ - $\pi$  stacking distance and thus improves the crystalline ordering of PEDOT domains, as demonstrated in Figure 4.

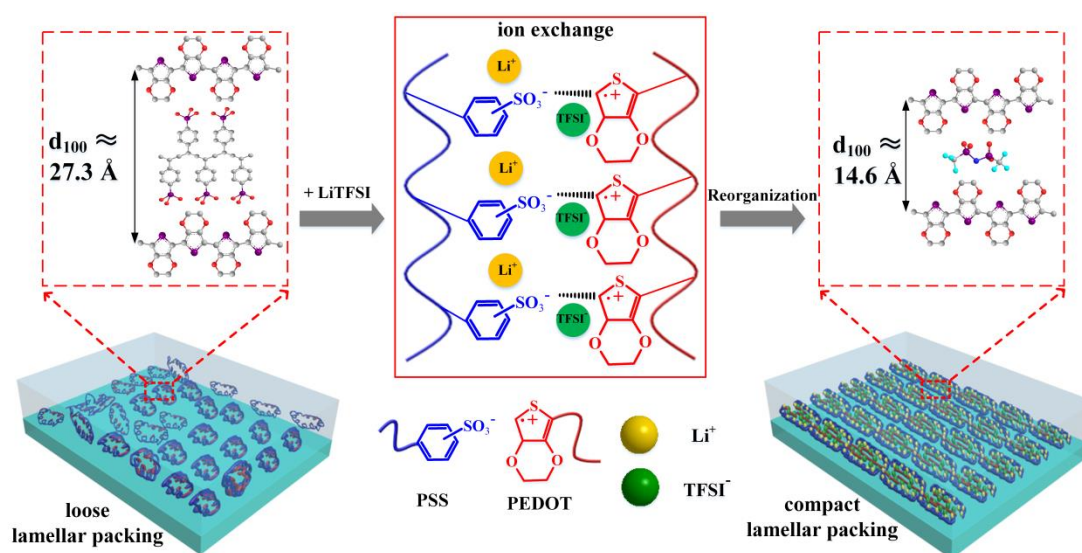


**Figure 4.** Schematic illustration of the structure of polymer composite film: loose lamellar packing of pristine PEDOT:PSS (left) and compacted lamellar packing of PEDOT:PSS /LiTFSI composite (right).

Figure 4 schematically demonstrates the structure change of PEDOT:PSS film before and after salt doping. In the pristine state, conducting PEDOT molecules are surrounded by insulating PSS molecules to form a stable colloidal dispersion in water<sup>26,29</sup> and a loose lamellar packing with periodicity of 27.3 Å formed in the dried film. With salt doping, the wrapped PEDOT molecules were released by ion exchange with salt to form a larger colloidal structure in water, as confirmed by the dynamic light scattering data (cf. Figure S6), which

1  
2  
3  
4 resulted in a compacted lamellar packing with periodicity of 14.6 Å after solvent evaporation  
5  
6 as indicated by the GISAXS and GIXRD data. These structural change as mentioned above  
7  
8 explains the 500-fold increase for the conductivity of PEDOT:PSS after doping with LiTFSI.  
9

10  
11  
12 In summary, we chose four salts with various cations but the same TFSI anion, to study  
13  
14 the effect of different cationic species on the structure and conductivity of PEDOT:PSS. The  
15  
16 conductivity measurement results revealed that salts with small-size cations endowed the  
17  
18 PEDOT:PSS much better conductivity. This phenomenon can be rationalized with the  
19  
20 GIWAXS and UV-Vis results: the molecular interactions among salt and PEDOT:PSS made  
21  
22 the structural rearrangement of the PEDOT to form ordered crystals and long-range ordered  
23  
24 conductive network, as well as the improved *p*-doped level of PEDOT resulted from  
25  
26 introducing secondary doping agents. These findings will provide in-depth knowledge about  
27  
28 how to manipulate the conductivity of PEDOT:PSS composite towards the applications in  
29  
30 printed soft electronics via molecular design and tuning the molecular assembly.  
31  
32  
33  
34  
35  
36  
37  
38

### 39 **Acknowledgement**

40  
41  
42 We acknowledge the financial supports from National Natural Science Foundation of  
43  
44 China (No. 11905306), Fundamental Research Funds for the Central Universities (No.  
45  
46 19lgpy14) and “100 Top Talents Program” of Sun Yat-sen University. A portion of this work is  
47  
48 based on the data obtained at 1W1A, BSRF, China. The authors gratefully acknowledge the  
49  
50 technical assistance of Dr. Yu Chen of Diffuse X-ray Scattering Stations during the beamtime.  
51  
52  
53  
54

### 55 **References**

- 56  
57 (1) Gao, M.; Li, L.; Song, Y., Inkjet printing wearable electronic devices. *J. Mater. Chem. C* **2017**, *5*  
58 (12), 2971-2993.  
59 (2) Wen, Z.; Yang, Y.; Sun, N.; Li, G.; Liu, Y.; Chen, C.; Shi, J.; Xie, L.; Jiang, H.; Bao, D., A  
60

- wrinkled PEDOT:PSS film based stretchable and transparent triboelectric nanogenerator for wearable energy harvesters and active motion sensors. *Adv. Funct. Mater.* **2018**, *28* (37), 1803684.
- (3) Huang, Q.; Zhu, Y., Printing conductive nanomaterials for flexible and stretchable electronics: A review of materials, processes, and applications. *Adv. Mater. Technol.* **2019**, *4* (5), 1800546.
- (4) Hui, Y.; Bian, C.; Xia, S.; Tong, J.; Wang, J., Synthesis and electrochemical sensing application of poly (3,4-ethylenedioxythiophene)-based materials: a review. *Anal. Chim. Acta* **2018**, *1022*, 1-19.
- (5) Kee, S.; Kim, N.; Park, B.; Kim, B. S.; Hong, S.; Lee, J. H.; Jeong, S.; Kim, A.; Jang, S. Y.; Lee, K., Highly deformable and see-through polymer light-emitting diodes with all-conducting-polymer electrodes. *Adv. Mater.* **2018**, *30* (3), 1703437.
- (6) Russ, B.; Glaudell, A.; Urban, J. J.; Chabinyk, M. L.; Segalman, R. A., Organic thermoelectric materials for energy harvesting and temperature control. *Nat. Rev. Mater.* **2016**, *1* (10), 1-14.
- (7) Palumbiny, C. M.; Liu, F.; Russell, T. P.; Hexemer, A.; Wang, C.; Müller-Buschbaum, P., The crystallization of PEDOT:PSS polymeric electrodes probed in situ during printing. *Adv. Mater.* **2015**, *27* (22), 3391-3397.
- (8) Kim, N.; Kee, S.; Lee, S. H.; Lee, B. H.; Kahng, Y. H.; Jo, Y. R.; Kim, B. J.; Lee, K., Highly conductive PEDOT:PSS nanofibrils induced by solution-processed crystallization. *Adv. Mater.* **2014**, *26* (14), 2268-2272.
- (9) Lang, U.; Müller, E.; Naujoks, N.; Dual, J., Microscopical investigations of PEDOT:PSS thin films. *Adv. Funct. Mater.* **2009**, *19* (8), 1215-1220.
- (10) Mukherjee, S.; Singh, R.; Gopinathan, S.; Murugan, S.; Gawali, S.; Saha, B.; Biswas, J.; Lodha, S.; Kumar, A., Solution-processed poly(3,4-ethylenedioxythiophene) thin films as transparent conductors: Effect of p-toluenesulfonic acid in dimethyl sulfoxide. *ACS Appl. Mater. Interfaces* **2014**, *6* (20), 17792-17803.
- (11) Mengistie, D. A.; Ibrahim, M. A.; Wang, P.-C.; Chu, C.-W., Highly conductive PEDOT: PSS treated with formic acid for ITO-free polymer solar cells. *ACS Appl. Mater. Interfaces* **2014**, *6* (4), 2292-2299.
- (12) Xia, Y.; Ouyang, J., Highly conductive PEDOT:PSS films prepared through a treatment with geminal diols or amphiphilic fluoro compounds. *Org. Electron.* **2012**, *13* (10), 1785-1792.
- (13) Lim, K.; Jung, S.; Lee, S.; Heo, J.; Park, J.; Kang, J.-W.; Kang, Y.-C.; Kim, D.-G., The enhancement of electrical and optical properties of PEDOT:PSS using one-step dynamic etching for flexible application. *Org. Electron.* **2014**, *15* (8), 1849-1855.
- (14) Lingstedt, L. V.; Ghittorelli, M.; Lu, H.; Koutsouras, D. A.; Marszalek, T.; Torricelli, F.; Crăciun, N. I.; Gkoupidenis, P.; Blom, P. W., Effect of DMSO Solvent Treatments on the Performance of PEDOT:PSS Based Organic Electrochemical Transistors. *Adv. Electron. Mater.* **2019**, *5* (3), 1800804.
- (15) Cui, H.-Q.; Peng, R.-X.; Song, W.; Zhang, J.-F.; Huang, J.-M.; Zhu, L.-Q.; Ge, Z.-Y., Optimization of ethylene glycol doped PEDOT:PSS transparent electrodes for flexible organic solar cells by drop-coating method. *Chin. J. Polym. Sci.* **2019**, *37* (8), 760-766.
- (16) Döbelin, M.; Marcilla, R.; Salsamendi, M.; Pozo-Gonzalo, C.; Carrasco, P. M.; Pomposo, J. A.; Mecerreyes, D., Influence of ionic liquids on the electrical conductivity and morphology of PEDOT:PSS films. *Chem. Mat.* **2007**, *19* (9), 2147-2149.
- (17) Armel, V.; Rivnay, J.; Malliaras, G.; Winther-Jensen, B., Unexpected interaction between PEDOT

- and phosphonium ionic liquids. *J. Am. Chem. Soc.* **2013**, *135* (30), 11309-11313.
- (18) Saxena, N.; Pretzl, B.; Lamprecht, X.; Bießmann, L.; Yang, D.; Li, N.; Bilko, C.; Bernstorff, S.; Müller-Buschbaum, P., Ionic liquids as post-treatment agents for simultaneous improvement of Seebeck coefficient and electrical conductivity in PEDOT:PSS Films. *ACS Appl. Mater. Interfaces* **2019**, *11* (8), 8060-8071.
- (19) Badre, C.; Marquant, L.; Alsayed, A. M.; Hough, L. A., Highly conductive poly(3,4-ethylenedioxythiophene):poly(styrenesulfonate) films using 1-ethyl-3-methylimidazolium tetracyanoborate ionic liquid. *Adv. Funct. Mater.* **2012**, *22* (13), 2723-2727.
- (20) Teo, M. Y.; Kim, N.; Kee, S.; Kim, B. S.; Kim, G.; Hong, S.; Jung, S.; Lee, K., Highly stretchable and highly conductive PEDOT:PSS/ionic liquid composite transparent electrodes for solution-processed stretchable electronics. *ACS Appl. Mater. Interfaces* **2016**, *9* (1), 819-826.
- (21) Liu, C.; Xu, J.; Lu, B.; Yue, R.; Kong, F., Simultaneous increases in electrical conductivity and Seebeck coefficient of PEDOT:PSS films by adding ionic liquids into a polymer solution. *J. Electron. Mater.* **2012**, *41* (4), 639-645.
- (22) Teo, M. Y.; RaviChandran, N.; Kim, N.; Kee, S.; Stuart, L.; Aw, K. C.; Stringer, J., Direct patterning of highly conductive PEDOT:PSS/ionic liquid hydrogel via microreactive inkjet printing. *ACS Appl. Mater. Interfaces* **2019**, *11* (40), 37069-37076.
- (23) Villanueva, M.; Coronas, A.; García, J.; Salgado, J., Thermal stability of ionic liquids for their application as new absorbents. *Ind Eng Chem Res* **2013**, *52* (45), 15718-15727.
- (24) Triolo, A.; Russina, O.; Fazio, B.; Appetecchi, G. B.; Carewska, M.; Passerini, S., Nanoscale organization in piperidinium-based room temperature ionic liquids. *J. Chem. Phys.* **2009**, *130* (16), 164521.
- (25) Singh, V. V.; Nigam, A. K.; Batra, A.; Boopathi, M.; Singh, B.; Vijayaraghavan, R., Applications of ionic liquids in electrochemical sensors and biosensors. *Int. J. Electrochem.* **2012**, *2012*.
- (26) Yue, W.; Zhu, C.; Pfattner, R.; Yan, H.; Jin, L.; Chen, S.; Molinalopez, F.; Lissel, F.; Jia, L.; Rabiah, N. I., A highly stretchable, transparent, and conductive polymer. *Sci. Adv.* **2017**, *3* (3), e1602076.
- (27) Luo, J.; Billep, D.; Waechtler, T.; Otto, T.; Toader, M.; Gordan, O.; Sheremet, E.; Martin, J.; Hietschold, M.; Zahn, D. R., Enhancement of the thermoelectric properties of PEDOT:PSS thin films by post-treatment. *J. Mater. Chem. A* **2013**, *1* (26), 7576-7583.
- (28) Li, Q.; Deng, M.; Zhang, S.; Zhao, D.; Jiang, Q.; Guo, C.; Zhou, Q.; Liu, W., Synergistic enhancement of thermoelectric and mechanical performances of ionic liquid LiTFSI modulated PEDOT flexible films. *J. Mater. Chem. C* **2019**, *7* (15), 4374-4381.
- (29) Li, Q.; Zhou, Q.; Wen, L.; Liu, W., Enhanced thermoelectric performances of flexible PEDOT:PSS film by synergistically tuning the ordering structure and oxidation state. *J. Materiomics* **2020**, *6*, 119-127.
- (30) Kee, S.; Kim, N.; Kim, B. S.; Park, S.; Jang, Y. H.; Lee, S. H.; Kim, J.; Kim, J.; Kwon, S.; Lee, K., Controlling molecular ordering in aqueous conducting polymers using ionic liquids. *Adv. Mater.* **2016**, *28* (39), 8625-8631.
- (31) de Izarra, A.; Park, S.; Lee, J.; Lansac, Y.; Jang, Y. H., Ionic liquid designed for PEDOT:PSS conductivity enhancement. *J. Am. Chem. Soc.* **2018**, *140* (16), 5375-5384.
- (32) Hofmann, A. I.; Katsigiannopoulos, D.; Mumtaz, M.; Petsagkourakis, I.; Pecastaings, G.; Fleury, G.; Schatz, C.; Pavlopoulou, E.; Brochon, C.; Hadziioannou, G., How to choose polyelectrolytes

- for aqueous dispersions of conducting PEDOT complexes. *Macromolecules* **2017**, *50* (5), 1959-1969.
- (33) Costa, L. T.; Sun, B.; Jeschull, F.; Brandell, D., Polymer-ionic liquid ternary systems for Li-battery electrolytes: Molecular dynamics studies of LiTFSI in a EMIm-TFSI and PEO blend. *J. Chem. Phys.* **2015**, *143* (2), 024904.
- (34) Hayamizu, K.; Aihara, Y.; Arai, S.; Martinez, C. G., Pulse-gradient spin-echo  $^1\text{H}$ ,  $^7\text{Li}$ , and  $^{19}\text{F}$  NMR diffusion and ionic conductivity measurements of 14 organic electrolytes containing LiN(SO<sub>2</sub>CF<sub>3</sub>)<sub>2</sub>. *J. Phys. Chem. B* **1999**, *103* (3), 519-524.
- (35) Stolwijk, N.; Obeidi, S., Combined analysis of self-diffusion, conductivity, and viscosity data on room temperature ionic liquids. *Electrochim. Acta* **2009**, *54* (5), 1645-1653.
- (36) Philippi, F.; Rauber, D.; Zapp, J.; Hempelmann, R., Transport properties and ionicity of phosphonium ionic liquids. *Phys Chem Chem Phys* **2017**, *19* (34), 23015-23023.
- (37) Shi, H.; Liu, C.; Jiang, Q.; Xu, J., Effective approaches to improve the electrical conductivity of PEDOT:PSS: a review. *Adv. Electron. Mater.* **2015**, *1* (4), 1500017.
- (38) Kim, G.-H.; Shao, L.; Zhang, K.; Pipe, K. P., Engineered doping of organic semiconductors for enhanced thermoelectric efficiency. *Nat. Mater.* **2013**, *12* (8), 719-723.
- (39) Bubnova, O.; Khan, Z. U.; Wang, H.; Braun, S.; Evans, D. R.; Fabretto, M.; Hojati-Talemi, P.; Dagnelund, D.; Arlin, J.-B.; Geerts, Y. H., Semi-metallic polymers. *Nat. Mater.* **2014**, *13* (2), 190-194.
- (40) Mazaheripour, A.; Majumdar, S.; Hanemann-Rawlings, D.; Thomas, E. M.; McGuinness, C.; d'Alencon, L.; Chabinye, M. L.; Segalman, R. A., Tailoring the Seebeck coefficient of PEDOT:PSS by controlling ion stoichiometry in ionic liquid additives. *Chem. Mater.* **2018**, *30* (14), 4816-4822.
- (41) Leaf, M. A.; Muthukumar, M., Electrostatic effect on the solution structure and dynamics of PEDOT:PSS. *Macromolecules* **2016**, *49* (11), 4286-4294.
- (42) Kee, S.; Kim, H.; Paleti, S. H. K.; El Labban, A.; Neophytou, M.; Emwas, A.-H.; Alshareef, H. N.; Baran, D., Highly stretchable and air-stable PEDOT:PSS/ionic liquid composites for efficient organic thermoelectrics. *Chem. Mater.* **2019**, *31* (9), 3519-3526.
- (43) Massonnet, N.; Carella, A.; Jaudouin, O.; Rannou, P.; Laval, G.; Celle, C.; Simonato, J.-P., Improvement of the Seebeck coefficient of PEDOT:PSS by chemical reduction combined with a novel method for its transfer using free-standing thin films. *J. Mater. Chem. C* **2014**, *2* (7), 1278-1283.
- (44) Lee, J.-g.; Cho, W.; Kim, Y.; Cho, H.; Lee, H.; Kim, J. H., Formation of a conductive overcoating layer based on hybrid composites to improve the stability of flexible transparent conductive films. *RSC Adv.* **2019**, *9* (8), 4428-4434.
- (45) Fabretto, M. V.; Evans, D. R.; Mueller, M.; Zuber, K.; Hojati-Talemi, P.; Short, R. D.; Wallace, G. G.; Murphy, P. J., Polymeric material with metal-like conductivity for next generation organic electronic devices. *Chem. Mater.* **2012**, *24* (20), 3998-4003.
- (46) Brooke, R.; Fabretto, M.; Krasowska, M.; Talemi, P.; Pering, S.; Murphy, P. J.; Evans, D., Organic energy devices from ionic liquids and conducting polymers. *J. Mater. Chem. C* **2016**, *4* (7), 1550-1556.
- (47) Zhang, P.; Rothkirch, A.; Koch, M.; Roth, S.; Kraus, T., Determination of the surface facets of gold nanorods in wet-coated thin films with grazing-incidence wide angle X-ray scattering. *Part*

- 1  
2  
3 *Part Syst Char* **2019**, 36 (12), 1900323.
- 4 (48) Zhang, P.; Huang, H.-y.; Chen, Y.; Yu, S.; Krywka, C.; Vayalil, S. K.; Roth, S. V.; He, T.-b.,  
5 Preparation of long-range ordered nanostructures in semicrystalline diblock copolymer thin films  
6 using micromolding. *Chin. J. Polym. Sci.* **2014**, 32 (9), 1188-1198.
- 7 (49) Müller-Buschbaum, P., The active layer morphology of organic solar cells probed with grazing  
8 incidence scattering techniques. *Adv. Mater.* **2014**, 26 (46), 7692-7709.
- 9 (50) Kim, N.; Lee, B. H.; Choi, D.; Kim, G.; Kim, H.; Kim, J.-R.; Lee, J.; Kahng, Y. H.; Lee, K., Role  
10 of interchain coupling in the metallic state of conducting polymers. *Phys Rev Lett* **2012**, 109 (10),  
11 106405.
- 12 (51) Rivnay, J.; Noriega, R.; Northrup, J. E.; Kline, R. J.; Toney, M. F.; Salleo, A., Structural origin of  
13 gap states in semicrystalline polymers and the implications for charge transport. *Phys Rev B* **2011**,  
14 83 (12), 121306.
- 15 (52) Bießmann, L.; Saxena, N.; Hohn, N.; Hossain, M. A.; Veinot, J. G.; Müller-Buschbaum, P.,  
16 Highly Conducting, Transparent PEDOT: PSS polymer electrodes from post-treatment with weak  
17 and strong acids. *Adv. Electron. Mater.* **2019**, 5 (2), 1800654.
- 18 (53) Petsagkourakis, I.; Pavlopoulou, E.; Portale, G.; Kuropatwa, B. A.; Dilhaire, S.; Fleury, G.;  
19 Hadziioannou, G., Structurally-driven enhancement of thermoelectric properties within  
20 poly(3,4-ethylenedioxythiophene) thin films. *Sci. Rep.* **2016**, 6, 30501.
- 21 (54) Lansac, Y.; Degrouard, J.; Renouard, M.; Toma, A. C.; Livolant, F.; Raspaud, E., A route to  
22 self-assemble suspended DNA nano-complexes. *Sci. Rep.* **2016**, 6, 21995.
- 23  
24  
25  
26  
27  
28  
29  
30  
31  
32  
33  
34  
35  
36  
37  
38  
39  
40  
41  
42  
43  
44  
45  
46  
47  
48  
49  
50  
51  
52  
53  
54  
55  
56  
57  
58  
59  
60